Published in final edited form as:
J Neuroimmunol. 2009 September 29; 214(1-2): 43–54. doi:10.1016/j.jneuroim.2009.06.016.

Mapping of the full length and the truncated interleukin-18 receptor alpha in the mouse brain

Silvia Alboni[1], **Davide Cervia**[2], **Brendon Ross**[3], **Claudia Montanari**[1], **Alejandro Sanchez Gonzalez**[3], **Manuel Sanchez-Alavez**[3], **Maria Cecilia Garibaldi Marcondes**[3], **David De Vries**[3], **Shuei Sugama**[4], **Nicoletta Brunello**[1], **Joan Blom**[5], **Fabio Tascedda**[1], and **Bruno Conti**[3]

[1] Department of Biomedical Sciences, University of Modena and Reggio Emilia, Italy

[2] Department of Environmental Sciences, University of Tuscia, Viterbo

[3] Harold L. Dorris Neurological Research Center, Molecular and Integrative Neurosciences Department, The Scripps Research Institute, CA, USA

[4] Department of Physiology, Nippon Medical School, Tokyo, Japan

[5] Department of Paediatrics, University of Modena and Reggio Emilia, Italy

Abstract

The cytokine IL-18 acts on the CNS both in physiological and pathological conditions. Its action occurs through the heterodimeric receptor IL-18Rα\β. To better understand IL-18 central effects, we investigated in the mouse brain the distribution of two IL-18Rα transcripts, a full length and an isoform lacking the intracellular domain hypothesized to be a decoy receptor. Both isoforms were expressed in neurons throughout the brain primarily with overlapping distribution but also with some unique pattern. These data suggest that IL-18 may modulate neuronal functions and that its action may be regulated through expression of a decoy receptor.

Keywords

Interleukin; receptor; IL-18; IL-18R; isoform; brain

1. INTRODUCTION

Interleukin (IL) 18 is a pro-inflammatory cytokine and a co-stimulator of interferon gamma production in T lymphocytes. IL-18 is also found in the central nervous system (CNS), where its expression has been demonstrated in activated microglia, ependymal cells of the third ventricle, as well as in neurons of the habenula (Conti et al., 1999; Prinz & Hanisch, 1999; Sugama et al., 2002). Work on IL-18 null mice, animals treated with IL-18, as well as data from humans, indicate that IL-18 is active in the CNS both in pathology and in physiology, participating in local inflammatory processes and also as a potential modulator of neuronal

Corresponding authors: Bruno Conti, Harold L. Dorris Neurological Research Center, Molecular and Integrative Neurosciences Department, The Scripps Research Institute, 10550 North Torrey Pines Road, La Jolla, California CA 92037, USA. bconti@scripps.edu. Fax +1 858 784 9099, Silvia Alboni, Department of Biomedical Sciences, University of Modena and Reggio Emilia, 287 Giuseppe Campi, 41 100 Modena, Italy. salboni@unimore.it. Fax +39 059 2055625.

function in various models. For instance, IL-18 has been shown to contribute, via microglia, to the clearance of neurovirulent influenza A virus, to neuronal loss in the MPTP (1-methyl-4-phenyl-1,2,3,6-tetrahydropyridine) model of Parkinson's disease and also to secondary tissue damage following stroke (Hedtjarn et al., 2002; Jander et al., 2002; Mori et al., 2001; Sugama et al., 2004; Sugama et al., 2007; Wheeler et al., 2003). In addition, the colocalization of IL-18 with amyloid-β-plaques and tau revealed a correlation between IL-18 gene polymorphisms and clinical outcome, suggesting a role for this molecule in Alzheimer's disease (Bossu et al., 2007; Ojala et al., 2009). Moreover, circulating or neocortical levels of IL-18 were elevated in psychiatric disorders including depression, panic attacks and schizophrenia (Kokai et al., 2002; Lu et al., 2004; Merendino et al., 2002; Tanaka et al., 2000). Evidence for a role of IL-18 as a modulator of neuronal function include the IL-18 mediated reduction of hippocampal long term potentiation (LTP) and NMDA receptor-mediated post synaptic potentials (Curran & O'Connor, 2001; Kanno et al., 2004), as well as the capability of IL-18 to centrally modulate appetite and sleep (Kubota et al., 2001; Netea et al., 2006; Zorrilla et al., 2007).

Peripherally, IL-18 action is mediated through binding to a specific receptor (IL-18R), a member of the interleukin-1 receptor/toll-like receptor superfamily. IL-18R is an heterodimer composed of one α subunit (IL-18Rα also known as IL-18RI, IL-1Rrp or IL- 1R5) that binds IL-18, and one β subunit (IL-18Rβ also known as IL-18RII, IL-18RAcP or IL-1R7) which initiates signal transduction recruiting the adapter protein myeloid differentiation factor 88 (MyD88) at their Toll/IL-1R (TIR) intracellular domain (Sergi & Penttila, 2004; Torigoe et al., 1997). Recent studies demonstrated the expression of IL-18Rα in the CNS (Andoh et al., 2008; Jeon et al., 2008), strongly supporting the hypothesis that IL-18 plays a direct role in physiological, as well as pathological, conditions in modulating the activity of cells of the CNS. Since the exact sites of central IL-18 action have not been fully explored we have investigated and presented here the distribution of the IL-18Rα in the mouse brain.

2. MATERIALS AND METHODS

2.1 Animals

Adult C57BL6/J mice were used in this study. Animals were housed in polycarbonate cages (28 × 17 × 12 cm) with *ad libitum* access to food and tap water throughout the study, and maintained under a 12:12 light-dark cycle in an ambient temperature of 21 ± 3 °C with relative humidity controlled. Animals were checked for signs of discomfort as indicated by animal care and use guidelines (National Academy of Sciences. Guide for the care and use of laboratory animals, 1998, "Guidelines for the Care and Use of Mammals in Neuroscience and Behavioral Research" (National Research Council 2003)), EC guidelines (EEC Council Directive 86/609 1987), Italian legislation on animal experimentation (Decreto Legislativo 116/92) were followed throughout the whole experiment. Procedures adhered to the National Institutes of Health Guide for the Care and Use of Laboratory Animals and were approved by The Scripps Research Institute Animal Care and Use Committee.

2.2 RT-PCR

Total RNA, extracted using TRIzol® reagent (Sigma®, St. Louis, MO, USA) was treated with a TURBO DNA-freeTM kit (Ambion®, Austin, TX, USA) to remove genomic DNA contamination. 1 μg of total RNA was reverse transcripted to cDNA using a High Capacity cDNA Kit (Applied Biosystems®, Foster City, CA, USA) in 50 μL of reaction mix. PCR-reactions were carried out using GoTaq® Flexi DNA polymerase (Promega Italia® Milan, Italy). The following primers were used: total IL-18Rα: CCA GCT ATT TTA GGA CCA AAG TGT and CTG TAA AGA CAT GGC CTG GG; type I IL-18Rα: GAG TAA CTG TGC TTG TTC TCG CCT CTG T and GGG TAA CGT CTC CAC AGC AAA AGT AT; type II IL-18Rα: GGC ACC CTA GCT CAT GTT TT and AGC ACA AGA CGT GTG AGG AGA;

GAPDH: CAA GGT CAT CCA TGA CAA CTT TG and GGG CCA TCC ACA GTC TTC TG. The number of PCR cycles was 40. GAPDH mRNA was measured as an internal control.

2.3 Riboprobes preparation

In order to examine total IL-18Rα and the two different isoforms (type I IL-18Rα and type II IL-18Rα) mRNAs in the CNS, we performed non-isotopic ISH using DIG-labeled riboprobes. We used sense probes of the complementary sequences as negative controls. Sections, which were incubated with sense digoxigenin-labeled cRNA probes, showed no hybridization signal (Fig. 3, sense lanes).

cDNA [nt 880–1334 (accession no. **NM_008365**)] – nt 796–1250 (accession no. **BC023240**) for total mouse IL-18Rα was subcloned into pCR®II-TOPO 4.0 kb (Invitrogen®, Paisley, UK) in order to obtain a template for the *in vitro* transcription of cRNA [antisense (using BamH I restriction site]; sense (Pst I using restriction site)]. cDNA [nt 1574–1960 (accession no. **NM_008365**)] for type I mouse IL-18Rα and cDNA [nt 1420–1659 (accession no. **BC023240**)] for type II mouse IL-18Rα were subcloned into pDrive Cloning Vector (Quiagen®, Hilden, Germany) in order to obtain templates for the *in vitro* transcription of cRNAs [antisense (using BamH I restriction site]; sense (using Hind III restriction site)]. Probes (antisense –AS- and sense –S-) for total IL-18Rα, type I IL-18Rα, and type II IL-18Rα, to be employed in *in situ* hybridization assays, were synthesized using the DIG-RNA labeling kit (La Roche Diagnostics, Mannheim, Germany) according to the manufacturer's instructions [T7 polymerase for total IL-18Rα AS probe or for type I and type II IL-18Rα S probes - SP6 polymerase for total IL-18Rα S probe or type I and type II IL-18Rα AS probes].

2.4 *In situ* hybridization

For *in situ hybridization* mice were anaesthetized by isoflurane inhalation and perfused transcardially with heparinized (5.000 U.I../L) saline followed by perfusion with ice-cold 4% paraformaldehyde in PBS pH 7.4. After fixation, their brains were rapidly removed and post fixed overnight in the same fixative solution, and then cryoprotected in a 30% sucrose solution in phosphate buffer pH 7.4. Brains were cut coronally in 40-μm serial sections by a cryostat, collected in Diethylpyrocarbonate (DEPC)-treated phosphate-buffered saline pH 7.4 (DEPC-PBS 1X) and washed 2 times (5 min each) in fresh DEPC-PBS 1X. Free floating sections were then treated 2 times (5 min each) with DEPC-treated PBS containing 100 mM glycine and then with DEPC-treated PBS containing 0,3% Triton X-100 (15 min). After washing 2 times (5 min each), sections were permeabilized at room temperature (10 min) with TE buffer (100mM Tris-HCl; 50mM EDTA pH8) preheated at 37°C containing 1μg/mL RNase-free Proteinase K. Sections were post-fixed (5 min) at 4°C with DEPC-treated PBS containing 4% paraformaldehyde (PFA), washed 2 times (5 min each) with DEPC-treated PBS and acetylated 2 times (5 min each) with 0.1M triethanolamine (TEA) buffer pH 8 containing 0,25% [v/v] acetic anhydride. Sections were then prehybridized at least 30 min at 37°C in prehybridization buffer (4XSSC containing 50% [v/v] deionized formamide; 1XSSC: 150mM NaCl, 15mM sodium citrate, pH7.2) and incubated overnight at 58°C in hybridization buffer containing 40% deionized formamide, 10% dextran sulphate, 1X Denhardt's solution [0,02% Ficoll, 0,02% polyvinylpyrrolidone, 0,2mg/mL RNase free bovine serum albumin], 4XSSC, 10mM DTT, 1mg/mL yeast t-RNA, 1mg/mL denaturated and sheared salmon sperm DNA and 30ng/slice of DIG-labeled RNA sense or antisense probe. After hybridization, the sections were washed 2 times (15 min each) at 37°C in 2X SSC, 2 times (15 min each) at 37°C in 1X SSC and incubated for 30 min at 37°C in NTE buffer (500mM NaCl, 10mM Tris-HCl pH8, 1 mM EDTA pH8, 20μg/mL RNase A) to digest any single-stranded RNA probes. After 2 washes (30 min each) at 37°C in 0,1X SSC followed by 2 washes of 10 min each in Buffer 1 (100mM Tris-HCl pH 7.5, 150mM NaCl), sections were pre-incubated in Blocking solution (Buffer 1 containing 0,1% Triton X-100 and 2% normal goat serum). For detection of Digoxigenin

(DIG), sections were incubated overnight at 4°C in 1% normal goat serum-Blocking solution containing anti-DIG alkaline phosphatase (Fab fragment) diluted 1:1000 (La Roche Diagnostics, Mannheim, Germany). Subsequently, sections were washed 2 times (10 min each) followed by a washing in Buffer 2 (100mM Tris-HCl pH9.5, 100mM NaCl, 50mM MgCl2). The chromogenic reaction was performed for 1–3 h at room temperature in the dark using a solution (100mM Tris-HCl pH9.5, 100mM NaCl) containing nitroblue tetrazolium (NBT) and 5-bromo-4-chloro-3-indolyl-phosphate (BCIP) and 1mM levamisole. The color reaction was stopped by incubation slices in Buffer 3 (10mM Tris-HCl pH8, 1mM EDTA pH 8) for several hours. Images were acquired through a digital AxioCam HRc color camera mounted on a AxioScope 40 (Zeiss) using AxionVision program.

2.5 Data analysis

The specificity of the hybridization signals in the brain regions were confirmed by comparing sections hybridized with antisense probes to those hybridized with respective sense probes. No hybridization signals were detectable in sections hybridized with sense probes. For each mRNA evaluated *in situ* hybridization with the antisense and the respective sense probe was performed at the same time, while, independent experiments were carried out for the different IL-18Rα isoforms. The relative intensities of the IL-18Rα mRNAs in various brain region were evaluated in hybridized coronal sections via transillumination microscopy. Anatomical brain regions were indentified by comparison with the mouse brain atlas in stereotaxic coordinates (Franklin and Paxinos, 1997). The anatomic nomenclature used in this study was based on this atlas. The staining intensities were rated into one of the following categories and are listed in table 1: −, not detectable; +/− very low signal; +, weak signal; +(++), a weak to moderate signal; ++, moderate signal; ++(+++) a moderate to strong signal; +++, strong signal. Since detection of type I and type II IL-18Rα was carried out with distinct probes with different specific activity the relative amount of the two isoforms cannot be extrapolated from these data. Figures were prepared by using Adobe Photoshop 7.0.1 with minor adjustments to contrast and brightness.

2.6 Immunohistochemistry

Mice were sacrificed upon perfusion with 0.2% EDTA-containing PBS, under isoflorane using an anesthetic machine. Brains were processed immediately after perfusion. Brains were removed and bisected in midsagittal plane, fixed in 10% formalin, embedded in paraffin, and cut into 5 μm sections. Following a 40 min 95°C steam bath in 10mM citrate buffer (pH6.38) for antigen retrieval, representative sections of brain (plus spleen controls) were immunohistochemically stained with two different anti IL18Rα antibodies Mab 1216, (R&D Systems, Minneapolis, MN) and sc-34178 (Santa Cruz Biotechnology Inc., Santa Cruz, CA). The antibodies were revealed with biotinylated anti-rat or anti goat IgG secondary antibodies (Vector Labs, Burlingame, CA), respectively, followed by streptavidin HRP (Invitrogen®, San Diego, CA) was developed by NovaRed (Vector Labs) and counterstained with Gill's hematoxylin (Invitrogen®). Images from cells were visualized and acquired using a Zeiss (Oberkochen, Germany) Axiovert 200 inverted microscope at 20 and 32x magnification and captured by using the Zeiss Axiocam HRC associated with Zeiss Axiovision 2.0.5 software package. Controls performed by omitting primary antibodies were negative.

3. RESULTS

3.1 Detection of type I and type II IL-18Rα transcripts

The gene encoding for mouse IL-18Rα was previously reported to be organized into 12 exons, with the start codon in exon 2 and the stop codon in exon 11, generating a canonical IL-18Rα (Parnet et al., 1996) (NCBI accession number NM_008365) (Fig. 1A and Fig. 1B). Data mining revealed the existence of at least another transcript for IL-18Rα (NCBI accession number

BC023240) (Strausberg et al., 2002). Sequence alignment demonstrated that this second transcript originates from differential splicing and redefined the size and sequence of exon 9 by adding 362 nucleotides to its 3′ end. These nucleotides were previously thought to be intronic (gt aat atg ctg ctg tga cag ggg cac cct agc tca tgt ttt tgt gcc tgc acc cag caa agg aaa gaa aca ctg gtc ttc ctt tta ttt gaa tga tcc cac taa tga tct ctg agc ctc gtt ccc agc ctg gag tca ggg gtt act ctg tgt ggg tta cac tga aac agg cga cat gca acc cta tac ttg ttt gtg aga aaa cag atg tgt ttc ttc tga tgt ctc atg tct gtg aac tgt ctc ctc aca cgt ctt gtg ctg tta gtc cga gtg tgt tta cac aca cac aca cac aca cac aca cac acc act aca cac tca aga aga cca ttt tat acc caa taa aat ttg ttt tta tt g) (Fig. 1A and 1B). This addition, together with the underlined stop codon, resulted in a transcript encoding for a 372 aa long peptide, identical to the extracellular and transmembrane portions of the canonical 537 aa peptide, but unique in its C terminal pentapeptide, ultimately lacking the intracellular TIR domain (Fig. 1C). The canonical and the truncated IL-18Rα isoforms were arbitrarily termed type I and type II IL-18Rα, respectively.

The expression of type I and type II IL-18Rα transcripts was first investigated by RT-PCR in several central and peripheral tissues. Both transcripts were detected in all tissues investigated, including particular areas of the brain such as the olfactory bulb, frontal cortex, striatum, hypothalamus, hippocampus, cerebral cortex and cerebellum, pituitary gland, as well as peripherally, in the spleen, adrenal gland, kidney, lung, muscle, heart and liver (Fig. 2).

3.2 Distribution of type I and type II IL-18Rα transcripts in the mouse brain

Distribution of IL-18Rα transcripts in the mouse brain was determined by *in situ* hybridization with sense and antisense riboprobes specific for the total as well as for the type I or the type II mRNAs (Fig. 3). An overall view of the distribution of IL-18Rα was presented in figure 3 while specific expression in the hippocampus was shown in figure 4 and for the cerebral cortex, hypothalamus and cerebellum in figure 5. A comprehensive summary of expression levels was presented in table I where the signal intensity of hybridization was used to estimate the degree of expression of each isoform in different brain regions. However, the degree of expression was not representative of the relative expression of type I versus type II isoform as their signal was obtained with different probes.

Total IL-18Rα was expressed throughout the brain, particularly in the limbic system, where high levels of expression were observed (Fig. 3A, 4A and 5A). In the forebrain, a strong hybridization signal was observed in the hippocampal formation (see below), in the olfactory bulbs (anterior olfactory nuclei and mitral cell layers), the amygdala and the cerebral cortex (see below). Lower levels of total IL-18Rα were found in the striatum (caudate-putamen and nucleus accumbens). In the diencephalon, an high total IL-18Rα hybridization signal was present in the epithalamus (lateral and medial habenula), and the thalamic nucleus with the highest signal in the anterior part of the paraventricular thalamic nucleus. Moderate to strong total IL-18Rα mRNA signal was also detectable in the hypothalamus (see below). In the midbrain, a weak to moderate total IL-18Rα mRNA signal was found in the superior colliculus (SuG, InG), in the midbrain motor related areas (SNR, VTA, PAG), and in the midbrain behavioural state related regions (SNC, RMg). A strong hybridization signal was found in the Purkinje cell layer (see below) and some cerebellar nuclei.

The signal for both type I and type II receptors was also found throughout the brain with a partial but not complete co-localization pattern (Fig. 3B, 3C). Overall total IL-18Rα and type I IL-18Rα mRNAs closely correlate in their distribution (Fig. 3B, 4B and 5B). Type II IL-18Rα was not as widely expressed as type I IL-18Rα (Fig. 3C, 4C and 5C), and its expression was highest in the habenula (MHb), the amygdala, the hippocampus (pyramidal cell layers and granular layer of the hippocampus) and the cerebral cortex (especially the piriform cortex) (see below).

3.2.1 Hippocampal formation—The hippocampus contained the relatively highest levels of IL-18Rα mRNAs (Fig. 4). A strong and abundant signal was present in the entire granule cell layer of the dentate gyrus (DG), and throughout the pyramidal cell layer of Ammon's horn (CA1–CA3). The staining was mainly confined to the cell body of neurons with few processes in CA1 for total IL-18Rα. A moderate to heavy staining was present in the subiculum (S, PrS and PaS) and the ectorhinal cortex (Ect) where several cell bodies showed darker staining for all the mRNAs investigated. Immunostaining was weak or absent in the stratum radiatum (Rad) and in the layers: lacunosum molecular (LMol), molecular (Mol) and oriens (Or) (Fig. 4).

3.2.2 Cerebral cortex—Strong neuronal-like total IL-18Rα staining was observed in the frontal association cortex, in the prelimbic cortex (FrA, PrL) and in the cingulate (Cg1, Cg2, RSG, RSA) cortex. Moderate to heavy total IL-18Rα staining was also observed in the remaining cerebral cortex (Fig. 3A). The distribution pattern of total IL-18Rα signal was different from that for type I or II mRNAs. In fact, total IL-18Rα mRNA was present in all layers of the cortex (Fig. 5A), while type I IL-18Rα was localized primarily in layers V and VI (Fig. 5B), and type II IL-18Rα mainly in layer V (Fig. 5C). In all cases the signal was localized primarily in pyramidal and non-pyramidal cortical cell bodies but not in their dendrites.

3.2.3 Hypothalamus—The relative distribution and intensity of total, type I or type II IL-18Rα in the hypothalamus differed in specific areas and nuclei. Total and type I IL-18Rα mRNAs were detected in the periventricular zone, specifically in the ventral part of the paraventricular nucleus (PaV) and in the arcuate nucleus (Arc) (Fig. 5A). Besides the high relative levels of type I 18Rα mRNA in the PaV and Arc (Fig. 5B), it was also present in the medial preoptic area and nucleus (MPA, MnPO), in the anterior area (AHA, AHP) and in the ventromedial (VMH, VMHDM, VMHC, VMHVL) (Fig. 5B) and in the premammillary (PMV, PMD) nuclei as well as in the medial mammillary nucleus (MM). The transcript for type II IL-18Rα was found to be less widespread than the type I and the total IL-18Rα mRNA in the hypothalamus with the exception of the preoptic region of the lateral zone where a particularly high signal was detected in the magnocellular preoptic nucleus (MCPC) and lateral preoptic area (LPO). Moreover, as observed for type I IL-18Rα mRNA, strong expression of type II IL-18Rα mRNA was detected in the ventromedial nuclei (mainly in the VHMDM) and in the Arc (Fig. 5C).

3.2.4 Cerebellum—The cell body of cerebellar Purkinje cells (P) showed dense staining for both the total and type I IL-18Rα transcripts (Fig 5A and 5B), whereas a very weak or no staining at all was observed for type II IL-18Rα mRNA in the Purkinje cells (Fig. 5C). The molecular (MOL) and the granular cell layers (GrL) of the cerebellar cortex exhibited low levels of labelling only for the total and type I IL-18Rα transcripts (Fig 5A and 5B) whereas no signal was detectable in the white matter (W) of the cerebellar cortex for each mRNAs evaluated (Fig. 5A, 5B and 5C).

3.3 Immunohistochemistry for IL-18Rα in the mouse brain

In order to confirm the expression of IL18Rα at the protein level, we performed an immunohistochemical analysis. We used two antibodies raised against different epitopes of the extracellular domain of the mouse IL-18Rα therefore not able to discriminate between the two isoforms. Similarly to the transcripts, the expression of IL18Rα was detected throughout the brain. IL18Rα immunoreactivity was found on neuronal cell bodies as well as on their dendrites (Fig. 6). Interestingly, cell body staining was tendentially stronger with sc-34178 (Fig. 6A, 6B, and 6C) than with Mab1216 (Fig. 6D and 6E), which showed a more intense staining of dendrites. Immunohistochemistry with secondary antibodies alone was negative (not shown). Importantly, we were able to confirm the expression of the receptor in the cortex,

particularly on layers IV and V (Fig. 6A and 6C), and in the hippocampus, where it was predominantly expressed on neuronal cell dendrites in the dentate gyrus (Fig. 6A), but also present in CA1, CA2 and CA3 (Fig. 6A and 6B). In the cerebellum (Fig. 6E), the pattern of IL18Rα expression was almost exclusively associated to the dendrites on Purkinje cells. In the anterior hypothalamus (Fig. 6D), IL18Rα specific staining was associated with both cell bodies and dendrites.

4. DISCUSSION

This is the first detailed and comprehensive study of IL-18Rα expression in the mouse brain. The main findings of the study are: 1. two IL-18Rα isoforms are expressed in the mouse brain; 2. both isoforms are expressed with partially overlapping distribution mainly in neurons.

Analyses of full-ORF cDNA sequences deposited at the National Center for Biotechnolgy Information and available in the Mammalian Gene Collection (MGC) database allowed prediction of a new isoform of IL-18Rα (Strausberg et al., 2002). We arbitrarily named the full-length (canonical), previously described (Parnet et al., 1996), and new predicted truncated isoform (Strausberg et al., 2002) type I and type II IL-18Rα, respectively. Both isoforms possess the domain required for IL-18 binding (Kato et al., 2003) and the transmembrane domains for cell surface expression. However, the type II IL-18Rα has a short 24 amino acids long C-terminal cytoplasmic tail (of which the last five amino acids were specific for this isoform) and lacked the cytoplasmic TIR domain required for MyD88-dependent signal transduction activation. In this respect, type II IL-18Rα is structurally similar to previously described decoy receptors such as the membrane IL-1RII that bind its ligand but fails to activate signal transduction (Colotta et al., 1993; Colotta et al., 1994; Malinowsky et al., 1998; Mantovani et al., 2001; Lang et al., 1998). Moreover, it has been proposed that decoy receptors can act as scavengers by mediating the internalization of their ligands by endocytosis (Bourke et al., 2003). Both mechanisms are regarded to be important regulators of the actions of the ligand. Although similar functions were not demonstrated for type II IL-18Rα, this sequence analysis suggests that this receptor may be a decoy and a regulator of IL-18 action. In this case, the type II IL-18Rα would participate with two other known negative modulators in the IL-18 system: the IL-18 binding protein and a truncated form of IL-18Rβ identified in the rat and human brain (Andre et al., 2003; Novick et al., 1999; Fiszer et al., 2007). Type I and type II receptors appear to originate by differential splicing of exon 9. However, alignment of the deposited sequences with genomic DNA showed that type I and type II IL-18Rα cDNAs differed also in their 5′ region, suggesting that the transcription of the two isoforms may be regulated by different promoters, perhaps independently, in distinct cell types or following different stimulation. The relative expression of both isoform was not investigated in the present study (the degree of expression in table I is arbitrarily indicative of regional distribution of each single isoform) but may be one mechanism regulating IL-18's actions.

In situ hybridization showed IL-18Rα transcripts in neuronal cell bodies, while immunohistochemical detection of the protein showed that its localization appeared to be primarily dendritic. In general, in the CNS, cytokines and their receptors are primarily found in glial cells and are investigated for their role in local inflammatory processes associated with pathological conditions rather than for their possible physiological role. In fact, IL-18 was previously demonstrated to be produced by and to be active on microglia *in vitro*, and subsequently it was proposed to participate in inflammatory-mediated neurodegeneration (Felderhoff-Mueser et al., 2005; Prinz & Hanisch, 1999). However, the recognition that IL-18Rα is expressed on neuronal cell types strongly suggested the possibility that IL-18 may not only participate in local inflammation, but directly modulate neuronal functions. Such an action may be similar to that previously demonstrated for IL-1β shown to have fast direct neuronal action through ceramide dependent Src kinase activation resulting in the NMDA

receptor-mediated calcium elevation (Davis et al., 2006; Sanchez-Alavez et al., 2006; Viviani et al., 2003).

The existence of a full length and a putative decoy receptor described here and the depiction of their relative distribution may help explain some of the observed central actions of IL-18. For instance, IL-18Rα was particularly abundant in the hippocampal system, a structure that plays major roles in memory and cognition. Multiple studies demonstrated a role for IL-18 in affecting LTP (Curran & O'Connor 2001; Cumiskey et al., 2007a; Cumiskey et al., 2007b) and basal hippocampal synaptic transmission (Kanno et al., 2004). Since IL-18Rα mRNA was expressed in the pyramidal cell bodies of Ammon's horn and granule cell layer of the dentate gyrus, it is possible that IL-18 may act directly on these neurons, moreover, its action may be regulated by the relative level of type I and type II receptors, both highly expressed in these cells.

The expression of IL-18Rα in the cerebral cortex may be relevant regarding the hypothesized contribution of IL-18 in psychiatric disorders (Kroes et al, 2006; Shirts et al, 2008). This expression suggests an involvement for this cytokine possibly similar to those described for other cytokines (e.g. IL-1 and IL-6) known to play a role in altering fetal brain development (Patterson, 2009). In this region, a unique pattern of expression was found because transcripts for total, type I and type II receptors appeared to be expressed differentially throughout the layers of the cerebral cortex. In particular, whereas the total IL-18Rα was expressed in all layers, the type I was mainly expressed in the internal pyramidal layer V and in the multiform layer VI, and type II mainly in the layer V. These findings suggest a specific role for the identified isoforms in the cortex and, more importantly, highlight the possibility that yet additional isoforms of the IL-18Rαs exist.

Both IL-18Rα isoforms were found in the thalamus and the hypothalamus, areas known to have multiple functions. The former has strong reciprocal connections with the cerebral cortex and is important, for example, in regulating states of sleep and wakefulness, while the latter is involved in many hormonal responses and in the control of homeostatic mechanisms. Recent studies have demonstrated that IL-18 may participate in homeostatic and pro-survival functions such as the regulation of the hypothalamic-pituitary-adrenal (HPA) axis activity (Sugama & Conti, 2008), induction of sleep (Kubota et al., 2001) and suppression of appetite (Netea et al., 2006; Zorrilla et al., 2007). The mechanisms through which IL-18 affects sleep and food-intake are largely unknown, but central action was proposed following the observation that intracerebroventricular injections of exogenous IL-18 induced sleep as well as anorexia (Kubota et al., 2001; Zorrilla et al., 2007). We found high levels of total and type I IL-18Rα mRNAs expression in the paraventricular and in the arcuate nucleus of the hypothalamus, thus supporting a direct role for IL-18 in mediating hormonal responses as well as feeding. Moreover, we detected an heavy signal of types I and II IL-18Rα mRNAs in the ventromedial hypothalamic nuclei involved in neuroendocrine control and satiety. The expression of the shorter form of the IL-18Rα was particularly high in the preoptic region of the lateral zone (in particular in the lateral preoptic area that plays a role in the regulation of thirst and sleep) (Saad et al., 1996; Schmidt et al., 2000) and in the magnocellular preoptic nucleus (that is important for example in controlling olfactory sensitivity and motivation) (Paolini & McKenzie, 1997; Wang & Swann, 2006) suggesting a complex role for IL-18 in controlling functions and behaviors that involve these areas and nuclei. The preoptic area of the hypothalamus is also known to be an important regulator of temperature homeostasis. The preferential presence of type II IL-18Rα mRNA in this region may help to explain some seemingly contradictory findings. Despite the similarity between the IL-18 and IL-1 systems including the activation of the same signaling, unlike IL-1β, IL-18 does not have the pyretic action, but rather appears to reduce IL-1β dependent fever effects of IL-1 (Gatti et al., 2002).

One hypothesis is that type II IL-18Rα may heterodimerize with IL-1RacP thus down-regulating functional IL-1R.

In this study, we confirmed the previously demonstrated expression of IL-18Rα in the Purkinje cells of the cerebellar cortex where the IL-18 system counteracts the effect of IL-1β in the induction of ataxia whit kainate (Andoh et al., 2008). Unlike in the preoptic area, it was not possible to explain the antagonizing action of IL-18 and IL-1β solely on the basis of the existence of a decoy receptor that, in addition, was barely detectable in this region.

In conclusion, we reported the central distribution of two isoforms of IL-18Rα, one canonical reportedly functional full length and one truncated with a putative decoy and regulatory function. We also showed that both forms are expressed in neurons, particularly localized on dendrites, strongly suggesting a direct action of IL-18 in mediating neuro-immune communication and modulating CNS functions.

Acknowledgments

Supportred by The Ellison Medical Foundation, HL088083 and AG028040, The Italian Board of Education (MIUR Internationalization)

ABBREVIATIONS

3V
: third ventricle

7
: facial nucleus

AAD
: anterior amygdaloid area dorsal part

AAV
: anterior amygdaloid area ventral part

Acb
: nucleus accumbens

ACo
: cortical amygdaloid nucleus anterior part

AD
: anterodorsal thalamic nuclei

AHA
: anterior hypothalamic area anterior part

AHC
: anterior hypothalamic area central part

AHiAL
: amygdalohippocampal area anterolateral part

AHiPM
: amygdalohippocampal area postmedial part

AHP
: anterior hypothalamic area posterior part

AI agranular insular cortex

Aint anterior interposed nucleus

AIP agranular insular cortex posterior part

AM anteromedial thalamic nuclei

AOD anterior olfactory nucleus dorsal part

AOL anterior olfactory nucleus lateral part

AOM anterior olfactory nucleus medial part

AOV anterior olfactory nucleus ventral part

APir amygdalopiriform transition area

APT anterior pretectal nucleus

Arc arcuate hypothalamic nucleus

Au1 primary auditory cortex

AuD auditory cortex dorsal part

AuV auditory cortex ventral part

AV anteroventral thalamic nuclei

AVPe anteroventral periventricular nucleus

BAOT bed nucleus of accessory olfactory tract

BLA basolateral amygdaloid nucleus anterior part

BLP basolateral amygdaloid nucleus posterior part

BLV basolateral amygdaloid nucleus ventral part

BMA
basomedial amygdaloid nucleus anterior part

BMP
basomedial amygdaloid nucleus posterior part

BST
bed nucleus of stria terminalis

CA
Ammon's horn

CA1
CA1 field of the hippocampus

CA2
CA2 field of the hippocampus

CA3
CA3 field of the hippocampus

CeC
central amygdaloid nucleus capsular division

CeL
central amygdaloid nucleus lateral division

CeM
central amygdaloid nucleus medial division

Cg1
cingulate cortex area 1

Cg2
cingulate cortex area 2

Circ
circular nucleus

CPu
caudate-putamen (striatum)

DC
dorsal cochlear nucleus

DEn
dorsal endopiriform nucleus

DG
dentate gyrus

DLG
dorsal lateral genicolate nucleus

DLO
dorsolateral orbital cortex

DM
dorsomedial hypothalamic nucleus

DMC dorsomedial hypothalamic nucleus compact part

DMD dorsomedial hypothalamic nucleus diffuse part

DMV dorsomedial hypothalamic nucleus ventral part

DP dorsal peduncular cortex

DpG deep gray layer of the superior colliculus

DpMe deep mesencephalic nucleus

DR dorsal raphe nucleus

DTM dorsal tuberomammillary nucleus

DTT dorsal tenia tecta

Ect ectorhinal cortex

EPI external plexiform layer of the olfactory bulb

EW Edinger- Westphal nucleus

FrA frontal association cortex

Gi gigantocellular reticular nucleus

GI granular insular cortex

Gl glomerular layer of the olfactory bulb

GrDG granular layer of the dentate gyrus

GrL granular cell layer of the cerebellar cortex

GrO granule layer of the olfactory bulb

HDB nucleus of the horizontal limb of the diagonal band

IG indusium griseum

IL infralimbic cortex

IMLF interstitial nucleus of the medial longitudinal fasciculus

InG intermediate gray layer of the superior colliculus

IPl internal plexiform layer of the olfactory bulb

La lateral amygdaloid nucleus

LA lateroanterior hypothalamic nucleus

Lat lateral (dentate) cerebellar nucleus

LEnt lateral entorhinal cortex

LH lateral hypothalamic area

LHb lateral habenular nucleus

LM lateral mammillary nucleus

LMol lacunosum molecular layer of the hippocampus

LO lateral orbital cortex

LOT nucleus of lateral olfactory tract

LPO lateral preoptic area

LSD lateral septal nucleus dorsal part

LSI lateral septal nucleus intermediate part

LSV lateral septal nucleus ventral part

M1 primary motor cortex

M2
secondary motor cortex

MCLH
magnocellular nucleus of the lateral hypothalamic area

MCPC
magnocellular nucleus of the posterior commissure

MCPO
magnocellular preoptic nucleus

MD
mediodorsal thalamic nucleus

Me
medial amygdaloid nucleus

ME
median eminence

Med
medial (fastgial) cerebellar nucleus

MHb
medial habenular nucleus

Mi
mitral cell layer of the olfactory bulb

ML
medial mammillary nucleus lateral part

MM
medial mammillary nucleus

MnPO
median preoptic nucleus

MnR
median raphe nucleus

MO
medial orbital cortex

Mol
molecular layer of the dentate gyrus

MOL
molecular layer of the cerebellar cortex

MPA
medial preoptic area

MPOC
medial preoptic nucleus central part

MPOL
medial preoptic nucleus lateral part

MPOM medial preoptic nucleus medial part

MS medial septal nucleus

MVe medial vestibular nucleus

Or oriens layer hippocampus

P Purkinje cell layer

PAG periaqueductal gray

PaDC paraventricular hypothalamic dorsal cap

PaLM paraventricular hypothalamic lateral magnocellular part

PaMM paraventricular hypothalamic medial magnocellular part

PaMP paraventricular hypothalamic medial parvicellular part

PaPO paraventricular hypothalamic nucleus posterior

PaS parasubiculum

PaV paraventricular hypothalamic nucleus ventral part

Pe periventricular hypothalamic nucleus

PF parafascicular thalamic nucleus

PH posterior hypothalamic area

Pir piriform cortex

PLCo posterolateral cortical amygdaloid nucleus

PMCo posteromedial cortical amygdaloid nucleus

PMD premammillary nucleus dorsal

PMV premammillary nucleus ventral part

PoDG polymorph layer dentate gyrus

PPtA posterior parietal association area

PRh perirhinal cortex

PrL prelimbic cortex

PrS presubicilum

PS parastrial nucleus

PT parataenial thalamic nucleus

PV paraventricular thalamic nucleus

PVA paraventricular thalamic nucleus anterior part

Py pyramidal cell layer of the hippocampus

Rad stratum radiatum of the hippocampus

RCh retrochiasmatic area

Re reuniens thalamic nuclei

RLi rostral linear nucleus raphe

RMC red nucleus magnocellular

RMg raphe magnus nucleus

RPC red nucleus parvocellular

RSA retrosplenial agranular cortex

RSG retrosplenial granular cortex

Rt reticular thalamic nucleus

S subiculum

S1 primary somatosensory cortex

S1FL S2, secondary somatosensory cortex

SchDM suprachiasmatic nucleus dorsomedial part

SchVL suprachiasmatic nucleus ventrolateral part

SI substantia innominata

SLu stratum lucidem of the hippocampus

SMT submammillothalamic nucleus

SNC substantia nigra compact part

SNL substantia nigra lateral part

SNR substantia nigra reticular part

SO supraoptic nucleus

Sp5ODM spinal 5 nucleus oral dorsomedial part

Sp5OVL spinal 5 nucleus oral ventrolateral part

STh subthalamic nucleus

SuG superficial gray superior colliculus

SuM supramammillary nucleus

SuMM supramammillary nucleus, medial part

SuVe superior vestibular nucleus

TC tuber cinereum area

TS triangular septal nucleus

Tu olfactory tubercle

V1B primary visual cortex binocular region

V1M primary visual cortex monocular region

V2L secondary visual cortex lateral part

V2ML secondary visual cortex mediolateral part

V2MM secondary visual cortex mediomedial part

VCP ventral cochlear nucleus posterior part

VDB nucleus of the vertical limb of the diagonal band

VL ventrolateral thalamic nucleus

VLG ventrolateral genicolate nucleus

VLPO ventrolateral preoptic nucleus

VM ventromedial thalamic nucleus

VMH ventromedial hypothalamic nucleus

VMHC ventromedial hypothalamic nucleus central part

VMHDM ventromedial hypothalamic nucleus dorsomedial part

VMHVL ventromedial hypothalamic nucleus ventrolateral part

VMPO ventromedial preoptic nucleus

VO ventral orbital cortex

VOLT
vascular organ of the lamina terminalis

VP
ventral pallidum

VPL
ventral posterolateral thalamic nucleus

VPM
ventral posteromedial thalamic nucleus

VTA
ventral tegmental area

VTM
ventral tuberomammillary nucleus

W
white matter

ZI
zona incerta

References

Andoh T, Kishi H, Motoki K, Nakanishi K, Kuraishi Y, Muraguchi A. Protective effect of IL-18 on kainate- and IL-1 beta-induced cerebellar ataxia in mice. J Immunol 2008;180:2322–2328. [PubMed: 18250441]

Andre R, Wheeler RD, Collins PD, Luheshi GN, Pickering-Brown S, Kimber I, Rothwell NJ, Pinteaux E. Identification of a truncated IL-18R beta mRNA: a putative regulator of IL-18 expressed in rat brain. J Neuroimmunol 2003;145:40–45. [PubMed: 14644029]

Bossu P, Ciaramella A, Moro ML, Bellincampi L, Bernardini S, Federici G, Trequattrini A, Macciardi F, Spoletini I, Di Iulio F, Caltagirone C, Spalletta G. Interleukin 18 gene polymorphisms predict risk and outcome of Alzheimer's disease. J Neurol Neurosurg Psychiatry 2007;78:807–811. [PubMed: 17299019]

Bourke E, Cassetti A, Villa A, Fadlon E, Colotta F, Mantovani A. IL-1 beta scavenging by the type II IL-1 decoy receptor in human neutrophils. J Immunol 2003;170:5999–6005. [PubMed: 12794127]

Colotta F, Re F, Muzio M, Bertini R, Polentarutti N, Sironi M, Giri JG, Dower SK, Sims JE, Mantovani A. Interleukin-1 type II receptor: a decoy target for IL-1 that is regulated by IL-4. Science 1993;261:472–475. [PubMed: 8332913]

Colotta F, Dower SK, Sims JE, Mantovani A. The type II 'decoy' receptor: a novel regulatory pathway for interleukin 1. Immunol Today 1994;15:562–566. [PubMed: 7848516]

Conti B, Park LC, Calingasan NY, Kim Y, Kim H, Bae Y, Gibson GE, Joh TH. Cultures of astrocytes and microglia express interleukin 18. Brain Res Mol Brain Res 1999;67:46–52. [PubMed: 10101231]

Cumiskey D, Pickering M, O'Connor JJ. Interleukin-18 mediated inhibition of LTP in the rat dentate gyrus is attenuated in the presence of mGluR antagonists. Neurosci Lett 2007a;412:206–210. [PubMed: 17123727]

Cumiskey D, Curran BP, Herron CE, O'Connor JJ. A role for inflammatory mediators in the IL-18 mediated attenuation of LTP in the rat dentate gyrus. Neuropharmacology 2007b;52:1616–1623. [PubMed: 17459425]

Curran B, O'Connor JJ. The pro-inflammatory cytokine interleukin-18 impairs long-term potentiation and NMDA receptor-mediated transmission in the rat hippocampus in vitro. Neuroscience 2001;108:83–90. [PubMed: 11738133]

Davis CN, Tabarean I, Gaidarova S, Behrens MM, Bartfai T. IL-1beta induces a MyD88-dependent and ceramide-mediated activation of Src in anterior hypothalamic neurons. J Neurochem 2006;98:1379–1389. [PubMed: 16771830]

Felderhoff-Mueser U, Schmidt OI, Oberholzer A, Bührer C, Stahel PF. IL-18: a key player in neuroinflammation and neurodegeneration? Trends Neurosci 2005;28:487–493. [PubMed: 16023742]

Fiszer D, Rozwadowska N, Rychlewski L, Kosicki W, Kurpisz M. Identification of IL-18RAP mRNA truncated splice variants in human testis and the other human tissues. Cytokine 2007;39:178–183. [PubMed: 17897836]

Franklin, KBJ.; Paxinos, G. The mouse brain in stereotaxic cooredinates. San Diego: Academic Press; 1997.

Gatti S, Beck J, Fantuzzi G, Bartfai T, Dinarello CA. Effect of interleukin-18 on mouse core body temperature. Am J Physiol Regul Integr Comp Physiol 2002;282:R702–R709. [PubMed: 11832389]

Hedtjarn M, Leverin AL, Eriksson K, Blomgren K, Mallard C, Hagberg H. Interleukin-18 involvement in hypoxic-ischemic brain injury. J Neurosci 2002;22:5910–9. [PubMed: 12122053]

Jander S, Schroeter M, Stoll G. Interleukin-18 expression after focal ischemia of the rat brain: association with the late-stage inflammatory response. J Cereb Blood Flow Metab 2002;22:62–70. [PubMed: 11807395]

Jeon GS, Park SK, Park SW, Kim DW, Chung CK, Cho SS. Glial expression of interleukin-18 and its receptor after excitotoxic damage in the mouse hippocampus. Neurochem Res 2008;33:179–184. [PubMed: 17710540]

Kanno T, Nagata T, Yamamoto S, Okamura H, Nishizaki T. Interleukin-18 stimulates synaptically released glutamate and enhances postsynaptic AMPA receptor responses in the CA1 region of mouse hippocampal slices. Brain Res 2004;1012:190–193. [PubMed: 15158178]

Kato Z, Jee J, Shikano H, Mishima M, Ohki I, Ohnishi H, Li A, Hashimoto K, Matsukuma E, Omoya K, Yamamoto Y, Yoneda T, Hara T, Kondo N, Shirakawa M. The structure and binding mode of interleukin-18. Nat Struct Biol 2003;10:966–971. [PubMed: 14528293]

Kokai M, Kashiwamura S, Okamura H, Ohara K, Morita Y. Plasma interleukin-18 levels in patients with psychiatric disorders. J Immunother 2002;25(Suppl 1):S68–S71. [PubMed: 12048354]

Kroes RA, Panksepp J, Burgdorf J, Otto NJ, Moskal JR. Modeling depression: social dominance-submission gene expression patterns in rat neocortex. Neuroscience 2006;137:37–49. [PubMed: 16289586]

Kubota T, Fang J, Brown RA, Krueger JM. Interleukin-18 promotes sleep in rabbits and rats. Am J Physiol Regul Integr Comp Physiol 2001;281:R828–R838. [PubMed: 11506998]

Lang D, Knop J, Wesche H, Raffetseder U, Kurrle R, Boraschi D, Martin MU. The type II IL-1 receptor interacts with the IL-1 receptor accessory protein: a novel mechanism of regulation of IL-1 responsiveness. J Immunol 1998;161:6871–6877. [PubMed: 9862719]

Lu LX, Guo SQ, Chen W, Li Q, Cheng J, Guo JH. Effect of clozapine and risperidone on serum cytokine levels in patients with first-episode paranoid schizophrenia. Di Yi Jun Yi Da Xue Xue Bao 2004;24:1251–1254. [PubMed: 15567770]

Malinowsky D, Lundkvist J, Layé S, Bartfai T. Interleukin-1 receptor accessory protein interacts with the type II interleukin-1 receptor. FEBS Lett 1998;429:299–302. [PubMed: 9662436]

Mantovani A, Locati M, Vecchi A, Sozzani S, Allavena P. Decoy receptors: a strategy to regulate inflammatory cytokines and chemokines. Trends Immunol 2001;22:328–336. [PubMed: 11377293]

Merendino RA, Di Rosa AE, Di Pasquale G, Minciullo PL, Mangraviti C, Costantino A, Ruello A, Gangemi S. Interleukin-18 and CD30 serum levels in patients with moderate-severe depression. Mediators Inflamm 2002;11:265–267. [PubMed: 12396479]

Mori I, Hossain MJ, Takeda K, Okamura H, Imai Y, Kohsaka S, Kimura Y. Impaired microglial activation in the brain of IL-18-gene-disrupted mice after neurovirulent influenza A virus infection. Virology 2001;287:163–170. [PubMed: 11504551]

Netea MG, Joosten LA, Lewis E, Jensen DR, Voshol PJ, Kullberg BJ, Tack CJ, van Krieken H, Kim SH, Stalenhoef AF, van de Loo FA, Verschueren I, Pulawa L, Akira S, Eckel RH, Dinarello CA, van den Berg W, van der Meer JW. Deficiency of interleukin-18 in mice leads to hyperphagia, obesity and insulin resistance. Nat Med 2006;12:650–656. [PubMed: 16732281]

Novick D, Kim SH, Fantuzzi G, Reznikov LL, Dinarello CA, Rubinstein M. Interleukin-18 binding protein: a novel modulator of the Th1 cytokine response. Immunity 1999;10:127–136. [PubMed: 10023777]

Ojala J, Alafuzoff I, Herukka SK, van Groen T, Tanila H, Pirttila T. Expression of interleukin-18 is increased in the brains of Alzheimer's disease patients. Neurobiol Aging 2009;30:198–209. [PubMed: 17658666]

Paolini AG, McKenzie JS. Intracellular recording of magnocellular preoptic neuron responses to olfactory brain. Neuroscience 1997;78:229–242. [PubMed: 9135103]

Patterson PH. Immune involvement in schizophrenia and autism: Etiology, pathology and animal models. Behav Brain Res. 2009Epub ahead of print

Parnet P, Garka KE, Bonnert TP, Dower SK, Sims JE. IL-1Rrp is a novel receptor-like molecule similar to the type I interleukin-1 receptor and its homologues T1/ST2 and IL-1R AcP. J Biol Chem 1996;271:3967–3970. [PubMed: 8626725]

Prinz M, Hanisch UK. Murine microglial cells produce and respond to interleukin-18. J Neurochem 1999;72:2215–2218. [PubMed: 10217305]

Saad WA, Luiz AC, De Arruda Camargo LA, Renzi A, Manani JV. The lateral preoptic area plays a dual role in the regulation of thirst in the rat. Brain Res Bull 1996;39:171–176. [PubMed: 8866693]

Sanchez-Alavez M, Tabarean IV, Behrens MM, Bartfai T. Ceramide mediates the rapid phase of febrile response to IL-1beta. Proc Natl Acad Sci U S A 2006;103:2904–2908. [PubMed: 16477014]

Schmidt MH, Valatx JL, Sakai K, Fort P, Jouvet M. Role of the lateral preoptic area in sleep-related erectile mechanisms and sleep generation in the rat. J Neurosci 2000;20:6640–6647. [PubMed: 10964969]

Sergi B, Penttila I. Interleukin 18 receptor. J Biol Regul Homeost Agents 2004;18:55–61. [PubMed: 15323361]

Shirts BH, Wood J, Yolken RH, Nimgaonkar VL. Comprehensive evaluation of positional candidates in the IL-18 pathway reveals suggestive associations with schizophrenia and herpes virus seropositivity. Am J Med Genet B Neuropsychiatr Genet 2008;147:343–350. [PubMed: 18092318]

Strausberg RL, Feingold EA, Grouse LH, Derge JG, Klausner RD, Collins FS, Wagner L, Shenmen CM, Schuler GD, Altschul SF, Zeeberg B, Buetow KH, Schaefer CF, Bhat NK, Hopkins RF, Jordan H, Moore T, Max SI, Wang J, Hsieh F, Diatchenko L, Marusina K, Farmer AA, Rubin GM, Hong L, Stapleton M, Soares MB, Bonaldo MF, Casavant TL, Scheetz TE, Brownstein MJ, Usdin TB, Toshiyuki S, Carninci P, Prange C, Raha SS, Loquellano NA, Peters GJ, Abramson RD, Mullahy SJ, Bosak SA, McEwan PJ, McKernan KJ, Malek JA, Gunaratne PH, Richards S, Worley KC, Hale S, Garcia AM, Gay LJ, Hulyk SW, Villalon DK, Muzny DM, Sodergren EJ, Lu X, Gibbs RA, Fahey J, Helton E, Ketteman M, Madan A, Rodrigues S, Sanchez A, Whiting M, Madan A, Young AC, Shevchenko Y, Bouffard GG, Blakesley RW, Touchman JW, Green ED, Dickson MC, Rodriguez AC, Grimwood J, Schmutz J, Myers RM, Butterfield YS, Krzywinski MI, Skalska U, Smailus DE, Schnerch A, Schein JE, Jones SJ, Marra MA, Mammalian Gene Collection Program Team. Generation and initial analysis of more than 15,000 full-length human and mouse cDNA sequences. Proc Natl Acad Sci U S A 2002;99:16899–16903. [PubMed: 12477932]

Sugama S, Cho BP, Baker H, Joh TH, Lucero J, Conti B. Neurons of the superior nucleus of the medial habenula and ependymal cells express IL-18 in rat CNS. Brain Res 2002;958:1–9. [PubMed: 12468024]

Sugama S, Wirz SA, Barr AM, Conti B, Bartfai T, Shibasaki T. Interleukin-18 null mice show diminished microglial activation and reduced dopaminergic neuron loss following acute 1-methyl-4-phenyl-1,2,3,6-tetrahydropyridine treatment. Neuroscience 2004;128:451–458. [PubMed: 15350655]

Sugama S, Fujita M, Hashimoto M, Conti B. Stress induced morphological microglial activation in the rodent brain: involvement of interleukin-18. Neuroscience 2007;146:1388–1399. [PubMed: 17433555]

Sugama S, Conti B. Interleukin-18 and stress. Brain Res Rev 2008;58:85–95. [PubMed: 18295340]

Tanaka KF, Shintani F, Fujii Y, Yagi G, Asai M. Serum interleukin-18 levels are elevated in schizophrenia. Psychiatry Res 2000;96:75–80. [PubMed: 10980328]

Torigoe K, Ushio S, Okura T, Kobayashi S, Taniai M, Kunikata T, Murakami T, Sanou O, Kojima H, Fujii M, Ohta T, Ikeda M, Ikegami H, Kurimoto M. Purification and characterization of the human interleukin-18 receptor. J Biol Chem 1997;272:25737–25742. [PubMed: 9325300]

Viviani B, Bartesaghi S, Gardoni F, Vezzani A, Behrens MM, Bartfai T, Binaglia M, Corsini E, Di Luca M, Galli CL, Marinovich M. Interleukin-1beta enhances NMDA receptor-mediated intracellular calcium increase through activation of the Src family of kinases. J Neurosci 2003;23:8692–8700. [PubMed: 14507968]

Wang J, Swann JM. The magnocellular medial preoptic nucleus I. Sources of afferent input Neuroscience 2006;141:1437–1456.

Wang N, Sugama S, Conti B, Teramoto A, Shibasaki T. Interleukin-18 mRNA expression in the rat pituitary gland. J Neuroimmunol 2006;173:117–125. [PubMed: 16460811]

Wheeler RD, Boutin H, Touzani O, Luheshi GN, Takeda K, Rothwell NJ. No role for interleukin-18 in acute murine stroke-induced brain injury. J Cereb Blood Flow Metab 2003;23:531–535. [PubMed: 12771567]

Zorrilla EP, Sanchez-Alavez M, Sugama S, Brennan M, Fernandez R, Bartfai T, Conti B. Interleukin-18 controls energy homeostasis by suppressing appetite and feed efficiency. Proc Natl Acad Sci U S A 2007;104:11097–11102. [PubMed: 17578927]

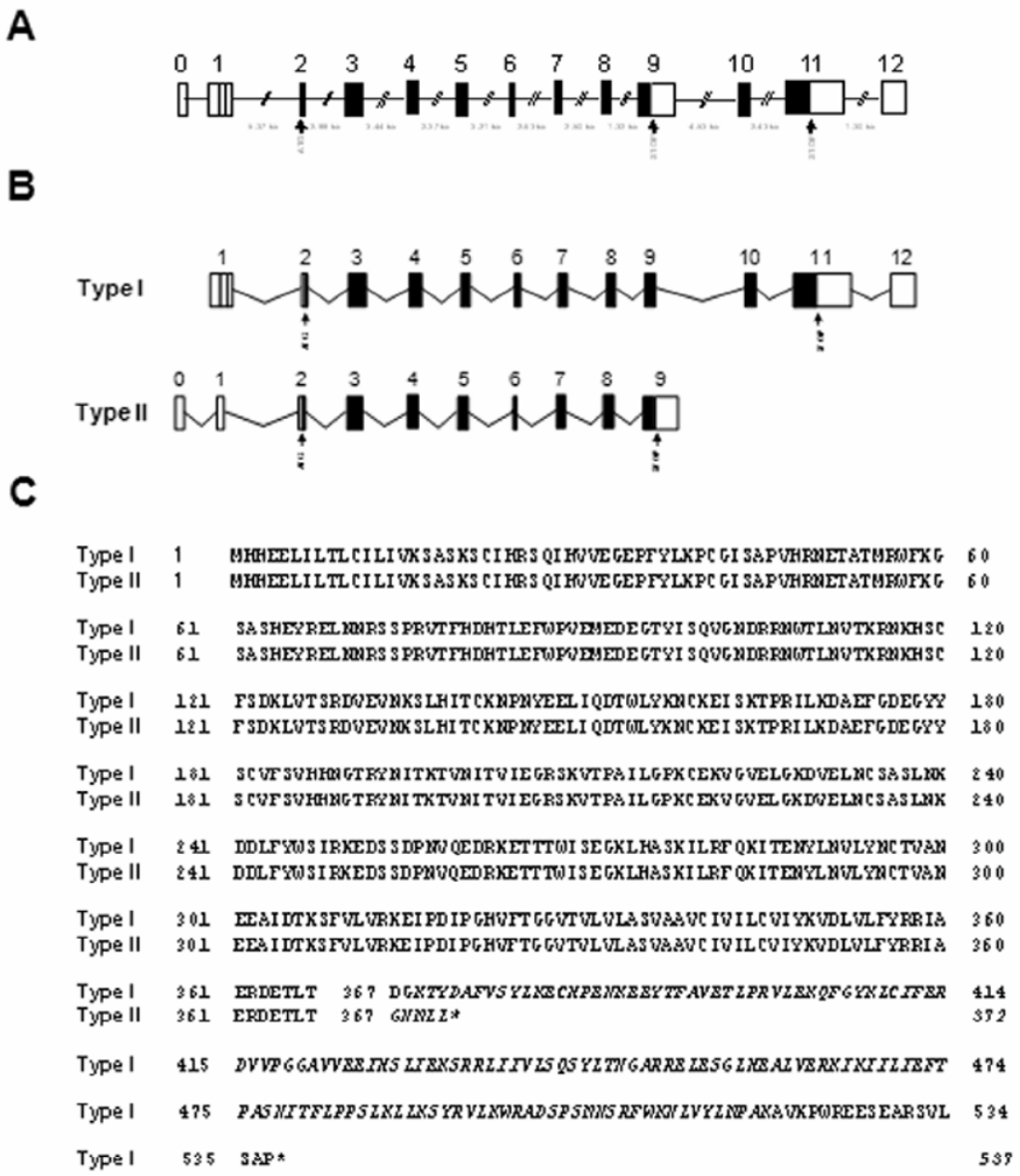

Figure 1. Exon/introne structure (A), alternative transcripts of mouse IL-18Rα gene (B) and alignment of the predicted amino acid sequences of type I IL-18Rα with type II IL-18Rα (C)

(A) Arrangement of exons and introns, drawn to scale, of mouse IL-18Rα gene structure as determined by analyzing genomic and mRNAs sequences. Exons are shown as boxes and introns are shown as lines. (B) Schematic representation of IL-18Rα transcripts in relation to the gene. Unranslated regions (UTR) are shown as empty boxes and coding sequences (CDS) are shown as black boxes. The putative translation initiation codon (ATG) and the termination codon (STOP) are also indicated. (C) Alignment of the amino acid sequences of the canonical and short isoforms with the predicted transmembrane regions underlined while specific type I or type II amino acid sequences are indicated in italic font.

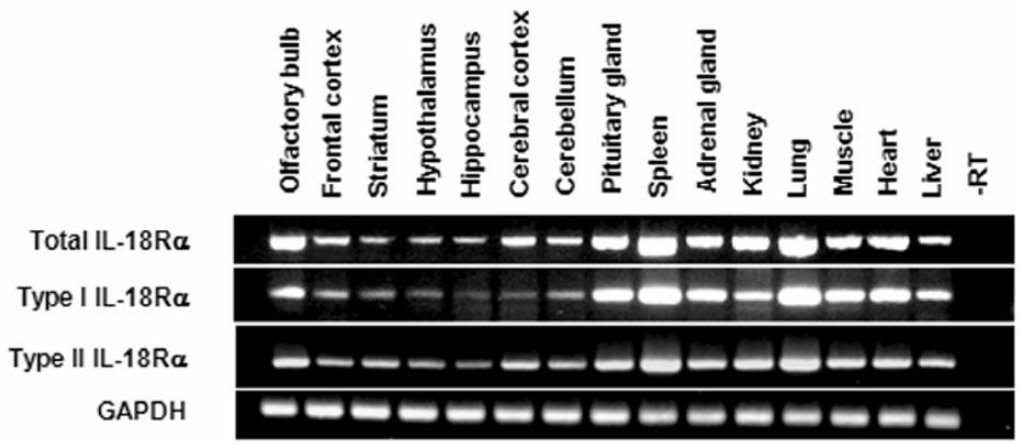

Figure 2. Qualitative RT-PCR confirms total, type I and type II IL-18Rα mRNAs expression in the mouse CNS and in selected peripheral tissues

GAPDH mRNA was measured as an internal control. The lengths of the expected PCR products were: 342 bp, 215 bp, 240 bp and 89 bp for total, type I, type II IL-18Rα and GAPDH respectively. Total RNA was extracted from brain areas and tissues of 3 mice and pooled before RT reaction.

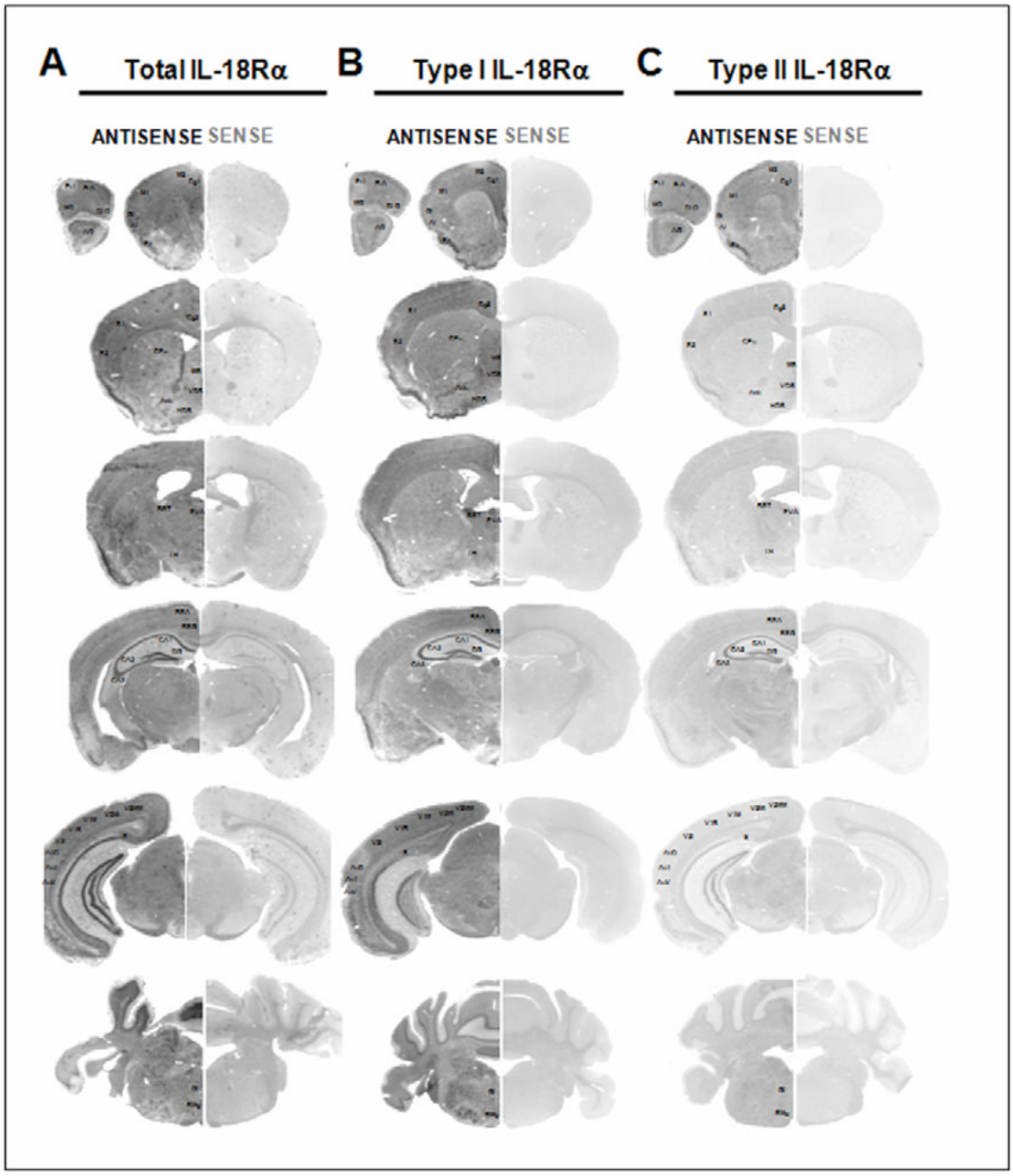

Figure 3. Distribution of the total (A) and type I (B) and type II (C) IL18-Rα mRNAs in a selected series of brain sections of C57BL6/J mice

Expression of the mRNAs of interest demonstrated by using *in situ* hybridization with a DIG-labeled antisense cRNA specific probes (ANTISENSE lanes) and using a sense cRNA probes (SENSE lanes) as a negative control. Section hybridized with the sense riboprobes showing the absence of hybridization signal (SENSE lanes). Acb, nucleus accumbens; AI, agranular insular cortex; AO, anterior olfactory nuclei; Au1, primary auditory cortex; AuD, auditory cortex, dorsal part; AuV, auditory cortex, ventral part; BST, bed nucleus of the stria terminalis; CA, Ammon's horn; CA1, CA1 field of the hippocampus; CA2, CA2 field of the hippocampus; CA3, CA3 field of the hippocampus; Cg1, cingulate cortex area 1; Cg2, cingulate cortex area

2; CPu, caudate-putamen; DG, dentate gyrus; DLO, dorsolateral orbital cortex; FrA, frontal association cortex; Gi, gigantocellular reticular nucleus; GI, granular insular cortex; HDB, nucleus of the horizontal limb of the diagonal band; LH, lateral hypothalamic area; M1, primary motor cortex; M2, secondary motor cortex; MO, medial orbital cortex; MS, medial septal nucleus; Pir, piriform cortex; PrL, prelimbic cortex; PVA, paraventricular thalamic nucleus anterior part; RMg, raphe magnus nucleus. RSA, retrosplenial agranular cortex; RSG, retrosplenial granular cortex; S, subiculum; S1, primary somatosensory cortex; S2, secondary somatosensory cortex; V1B, primary visual cortex, binocular region; V1M, primary visual cortex, monocular region; V2L, secondary visual cortex, lateral part; V2ML, visual cortex 2, mediolateral part; V2MM, visual cortex 2, mediodedial part; VDB, nucleus of the vertical limb of the diagonal band.

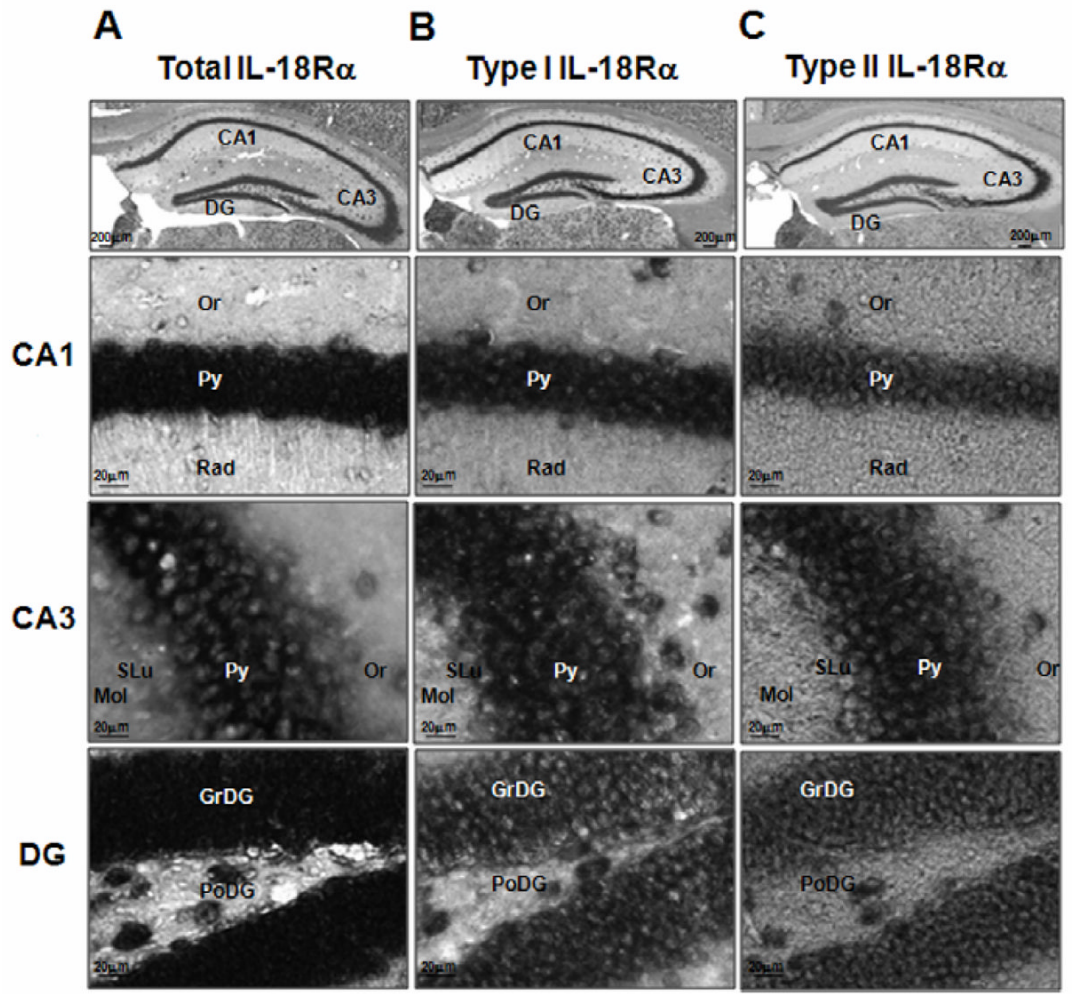

Figure 4. Localization of the total (A), type I (B) and type II (C) IL-18Rα mRNAs hybridization signal in the hippocampus of C57BL6/J mice

Shown are representative coronal brain sections at the level of the dorsal hippocampus exhibiting *in situ* hybridization with the indicated digoxigenin-labeled riboprobes. CA1: CA1 field of the hippocampus, CA3: CA3 field of the hippocampus, DG: dentate gyrus, Or: oriens layer of the hippocampus, Py: pyramidal cell layer of the hippocampus, Rad: stratum radiatum of the hippocampus, SLu: stratum lucidem of the hippocampus, Mol: molecular layer of the dentate gyrus, GrDG: granular layer of the dentate gyrus, PoDG: polymorph layer of the dentate gyrus.

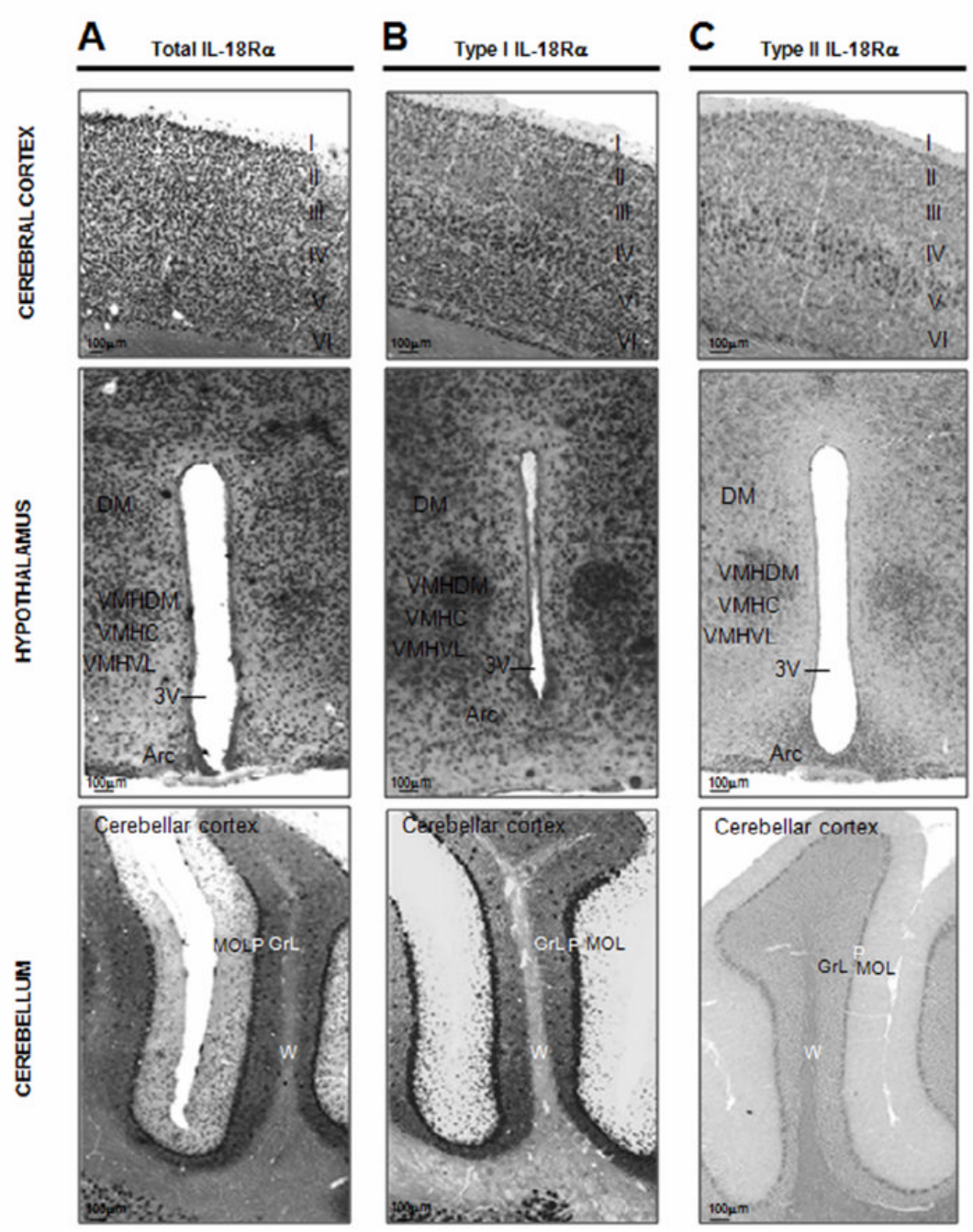

Figure 5. Distribution of the total (A), type I (B) and type II (C) IL-18Rα mRNAs in the cerebral cortex, in the hypothalamus and in the cerebellum of C57BL6/J mice

Upper panel shows distribution of the total (A), type I (B) and II (C) IL-18Rα mRNAs in the somatosensory cortex of C57BL6/J mice demonstrated with a DIG-labeled antisense cRNA probes- I: molecular layer, II: external granular layer, III external pyramidal layer, IV: internal granular layer, V: internal pyramidal layer, VI: multiform layer; medium panel shows distribution of the total (A), type I (B) and II (C) IL-18Rα mRNAs in the hypothalamus of C57BL6/J mice demonstrated with a DIG-labeled antisense cRNA probes. DM: dorsomedial hypothalamic nucleus, VMHC: ventromedial hypothalamic nucleus central part, VMHDM: ventromedial hypothalamic nucleus dorsomedial part, VMHVL: ventromedial hypothalamic

nucleus ventrolateral part, 3V: third ventricle, Arc: arcuate hypothalamic nucleus; lower panel shows distribution of the total (A), type I (B) and II (C) IL-18Rα mRNAs in the cerebellar cortex of the cerebellum of C57BL6/J mice demonstrated with a DIG-labeled antisense cRNA probes- MOL: molecular layer, P: Purkinje cell layer, GrL: granular layer, W: white matter, of the cerebellar cortex.

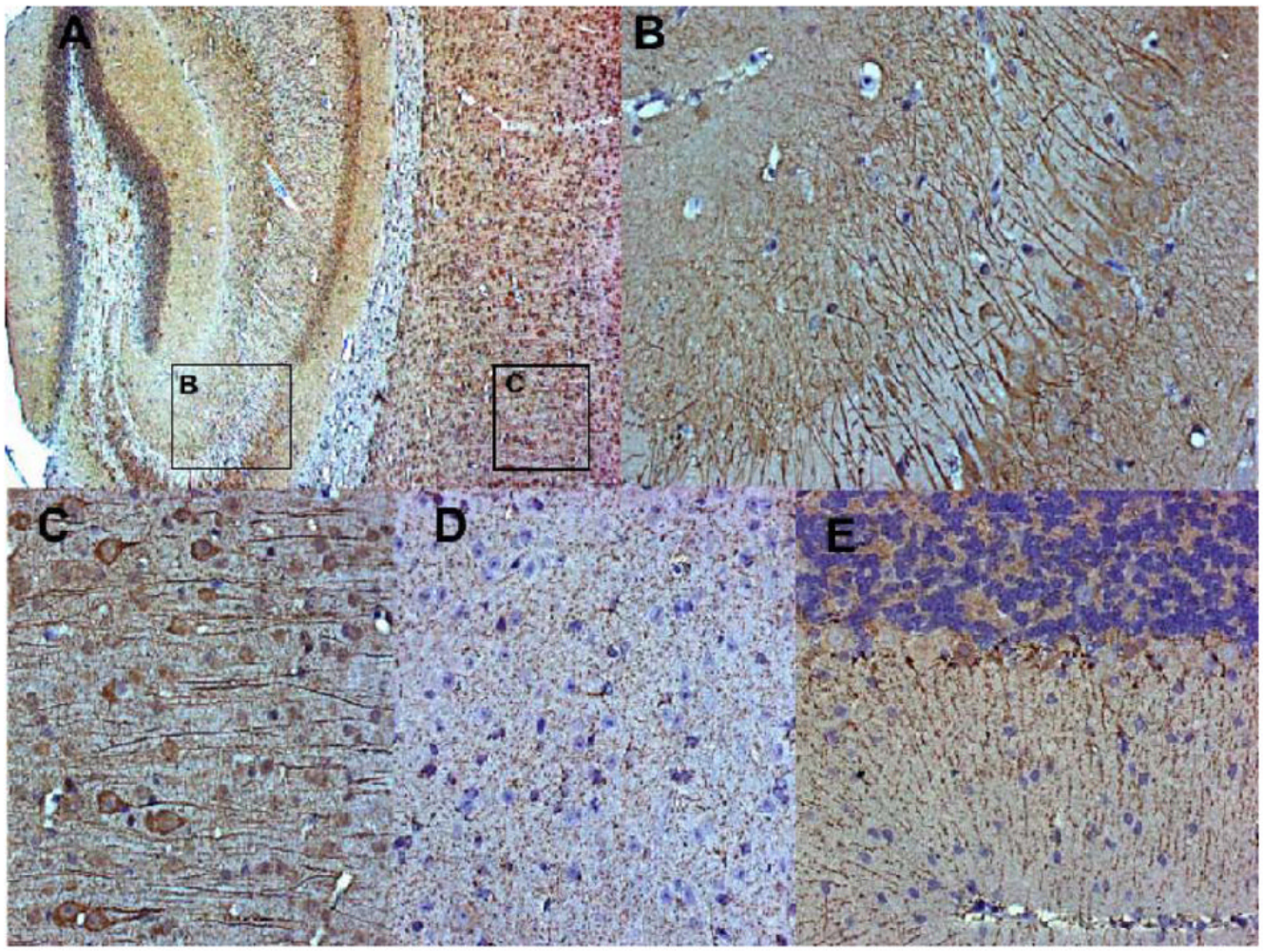

Figure 6. Immunohistochemical detection of IL-18Rα

Animals were perfused, the brains were harvestedand embedded in paraffin. The IL-18Rα receptor was detected using Mab 1216 (R&D) on 5 μm sections. Negative controls were performed by omitting the primary antibody, confirming the specificity of the antibody binding. (A), (B) and (C) Staining pattern using antibody sc-34178, showing predominantly neuronal cell bodies. (D) and E) Staining pattern using antibody Mab 1216, showing mostly dendrites. (A) Specific staining (brown color) on cortex and hippocampus (8x magnification). Rectangles indicate areas presented in detail in (B) and (C); (B) IL18Ra-positive cells (dark brown) in the dentate gyrus (DG) (32x); (C) Cortical detail, revealing a staining pattern associated to cell bodies and predominantly dendrites (32x). (D) Detailed view of neurons in the anterior hypothalamus (32x), and (E) cerebellum, showing positive cells (brown), associated exclusively to dendrites on Purkinje cells (20x).

Table 1

Expression of type I and type II IL-18Rα isoforms in the adult mouse brain

The relative intensity of the mRNAs in the different brain region was evaluated as described in Material and Methods (2.5 Data analysis). The *in situ* hybridization experiment for each mRNA evaluated was performed separately; experimental conditions were optimized for each probe according to its length and GC content. The data reported in the table for each mRNA can not be compared among the different IL-18Rα isoforms but only within the different brain regions for each isoform.

Area/nucleus	**type I IL-18Rα**	**type II IL-18Rα**
Telencephalon		
Cerebral Cortex		
Orbitofrontal cortex		
FrA	++(+++)	++(+++)
DLO	++/+++	+++
MO	++(+++)	++(+++)
LO	++(+++)	+++
VO	++(+++)	++(+++)
PrL	+++	++(+++)
Motor cortex		
M1	++(+++)	++
M2	++(+++)	++
Cingulate cortex		
Cg1	++(+++)	++(+++)
Cg2	++(+++)	++
RSG	++	++
RSA	++	++
Insular cortex		
GI	+++	++(+++)
AI	++	++
AIP	++	+
IL	++	++
DP	+++	+
Somatosensory cortex		
S1	++	++
S2	++	++

Area/nucleus	type I IL-18Rα	type II IL-18Rα
Auditory cortex		
Au1	++	++
AuD	++	++
AuV	++	++
Rhinal cortex		
Ect	++	+(++)
PRh	++	++
Lent	++	+
Visual cortex		
V1M; V1B	++	++
V2L; V2ML	++	++
V2MM	++	++
PptA	++	++
Olfactory system		
GI	–	–
EPI	–	–
Mi	++(+++)	++
IPI	++	–
GrO	++	–
AOD	++(+++)	++(+++)
AOL	++(+++)	++(+++)
AOM	++	+(++)
AOV	++	+(++)
DTT	++(+++)	++(+++)
Tu	+/–	–
Pir	+++	++(+++)
DEn	++	+(++)
Hippocampal formation		
IG	+++	+++
CA1; CA2; CA3		
Or	+/–	+/–

Area/nucleus	type I IL-18Rα	type II IL-18Rα
Py	+++	+++
LMol	–	–
SLu	++	++
Rad	+/–	+/–
DG		
GrDG	+++	+++
Mol	–	–
PoDG	++	+
S		
PrS; PaS	+	+
Basal ganglia		
Acb	+	+/–
Cpu	+/–	+
VP	++(+++)	+/– (+)
Amygdala		
AAD	++	++
AAV	++	++
APir	+(++)	+/–
LOT	++	+(++)
BST	++	+
BAOT	++	+
AHiAL	++	+
AHiPM	++(+++)	+
ACo	++	+
PLCo	++	++
PMCo	++	+
CeC; CeL; CeM	++	+
BLA	+++	+++
BLP	++	++
BLV	++	+
BMA	+++	+

Area/nucleus	type I IL-18Rα	type II IL-18Rα
BMP	++	++
La	++	++
Me	++(+++)	+
Septum		
LSD	++	+
LSI	++(+++)	+
LSV	++	+
MS	++	++
VDB	++	++
HDB	++	+
TS	+	–
Diencephalon		
Epithalamus, thalamus and subthalamus		
MHb	++(+++)	+++
LHb	++	++
Rt	++(+++)	+
PF	+(++)	+(++)
Re	++	+
Anterior thalamic nuclei		
AD	+++	++
AV	++	++
AM	++	++
PV	+++	+(++)
PVA	+++	++
MD	++	+(++)
PT	++	++
Lateral thalamic nuclei		
VL	+	+
VM	+	+
VPL	+	+(++)
VPM	+	+(++)

Area/nucleus	type I IL-18Rα	type II IL-18Rα
Posterior thalamic nuclei		
DLG	++	++
VLG	+	++
SI	+	+/−
ZI	++(+++)	+
STh	++(+++)	++
Hypothalamus		
Preoptic region		
LPO	++	+++
MCPO	++	+++
SO	+	−
PS	+	+
MPA	+++	++
MPOC	++	+(++)
MPOM	++	+(++)
MPOL	++	+(++)
AVPe	+++	++
Pe	++	+/−
MnPO	+++	+(++)
SChVL	++	+(++)
SChDM	++	+(++)
VMPO	+++	+++
VLPO	+++	+(++)
VOLT	++	+/−
Anterior region		
LH	++	+(++)
AHA	+++	+(++)
AHC	+++	+(++)
AHP	+++	++
RCh	+	+
Circ	++	+(++)

Area/nucleus	type I IL-18Rα	type II IL-18Rα
LA	++	++
PaLM	++	+
PaDC	++	+
PaMP	+	+
PaMM	++	+
PaV	+++	+
PaPO	+	++(+++)
Tuberal region		
MCLH	+	+
DM	++	+
DMD	++	+
DMC	++	+
DMV	++	+
VMH	+++	++
VMHDM	+++	+++
VMHC	++(+++)	++(+++)
VMHVL	++(+++)	++(+++)
TC	++	++
Arc	+++	++
Mammillary region		
SMT	++	+
SuMM	++	+(++)
SuM	+/–	+(++)
VTM	++	++
PH	++	–
DTM	++	+
PMD	+++	+/–
PMV	+++	+/–
LM	+	++
ML	++	+
MM	+++	++

Area/nucleus	type I IL-18Rα	type II IL-18Rα
ME	+	+
Mesenchephalon		
SuG	++	+/–
InG	++	+/–
DpG	+	+/–
PAG	++	+
IMLF	++	+
APT	+	+
DpMe	+	+
RPC	++	++
RMC	++	++
DR	+	+
MnR	+	+
RLi	++	+
SNR	++	+
SNC	++	+
SNL	++	+
VTA	+	+
EW	+(++)	+(++)
RMg	++	–
Rhomboencephalon		
Medulla oblongata		
SuVe	+	+/–
Mve	++(+++)	+
VCP	+	+
DC	++	+/–
Sp5ODM	++	+/–
Sp5OVL	++	+/–
Facial Nu 7	++	+
Gi	++(+++)	+
Cerebellum		

Area/nucleus	type I IL-18Rα	type II IL-18Rα
Deep cerebellar nuclei		
Lat; Med; Aint	++	+
Cerebellar cortex		
MOL	+	−
P	+++	+
GrL	+	−

Labelling intensity scale: −, not detected; +/− very low signal; +, weak signal; +(++) a weak to moderate signal; ++, moderate signal; ++(+++) a moderate to strong signal; +++, strong signal for IL-18Rα mRNAs